



TITLE:

Fabrication of CsPbBr Thick Films by Using a Mist Deposition Method for Highly Sensitive X-ray Detection

AUTHOR(S):

Haruta, Yuki; Ikenoue, Takumi; Miyake, Masao;
Hirato, Tetsuji

CITATION:

Haruta, Yuki ...[et al]. Fabrication of CsPbBr Thick Films by Using a Mist Deposition Method for Highly Sensitive X-ray Detection. MRS Advances 2020, 5(8-9): 395-401

ISSUE DATE:

2020-01-13

URL:

<http://hdl.handle.net/2433/252434>

RIGHT:

This article has been published in a revised form in MRS Advances <http://doi.org/10.1557/adv.2020.8>. This version is free to view and download for private research and study only. Not for re-distribution or re-use. © Materials Research Society 2020.; The full-text file will be made open to the public on 13 July 2020 in accordance with publisher's 'Terms and Conditions for Self-Archiving'; This is not the published version. Please cite only the published version.; この論文は出版社版ではありません。引用の際には出版社版をご確認ご利用ください。



Fabrication of CsPbBr₃ Thick Films for Highly Sensitive X-ray Detection Using a Mist Deposition Method

Yuki Haruta¹, Takumi Ikenoue¹, Masao Miyake¹ and Tetsuji Hirato¹

¹Graduate School of Energy Science, Kyoto University Kyoto, 606-8501, Japan

Abstract

X-ray imaging is an important technique used for medical imaging and non-destructive inspection of industrial products. Highly sensitive X-ray detectors which enable X-ray imaging at low dose rate are required to reduce the risk of cancer. Recently, metal halide perovskite materials have demonstrated excellent X-ray detection performance including high sensitivity due to their high absorption coefficient, high carrier mobility, and long carrier lifetime. However, there are few studies on perovskite thick films with large area which is essential for the application to X-ray imaging devices. In this study, a polymer is employed as a buffer layer to avoid a film exfoliation, which makes it difficult to fabricate perovskite thick films, and a 110- μm -thick CsPbBr₃ film is successfully obtained using a scalable solution method. In addition, an X-ray detector based on the CsPbBr₃ thick film is fabricated and achieves a high sensitivity of 11,840 $\mu\text{C Gy}_{\text{air}}^{-1} \text{cm}^{-2}$. This sensitivity is about 600 times higher than that of currently commercial a-Se X-ray detectors.

INTRODUCTION

Metal halide perovskite material (ABX₃, A = CH₃NH₃⁺, HC(NH₂)₂⁺, Cs⁺, Rb⁺; B = Pb²⁺, Sn²⁺; X = Cl⁻, Br⁻, I⁻) has a great potential as a photoconductive layer for solar cells[1]–[6] and visible light detectors[7]–[10] due to its high absorption coefficient, high carrier mobility, long carrier lifetime, and tunable band-gaps. Recently, perovskite materials have also demonstrated excellent X-ray detection performance[11]–[17]. Representative studies on X-ray detectors based on perovskite materials are summarized in Table I. For example, W. Wei et al. reported Si-integrated CH₃NH₃PbBr₃ single crystal X-ray detectors with the high sensitivity of 21,000 $\mu\text{C Gy}_{\text{air}}^{-1} \text{cm}^{-2}$, which is over a thousand times higher than that of amorphous selenium (a-Se) detectors[13]. Y. C. Kim et al. successfully obtained a hand phantom X-ray image from CH₃NH₃PbI₃ thick film-based

flat panel detectors with the sensitivity of $11,000 \mu\text{C Gy}_{\text{air}}^{-1} \text{cm}^{-2}$ [14]. However, poor thermal stability caused by the volatility of the organic cations is still a big issue[18]. In contrast, all-inorganic perovskite materials, especially cesium lead tribromide (CsPbBr_3), have demonstrated excellent thermal stability, and thus they are often used for stable perovskite-based devices including X-ray detectors[19], [20]. Z. Gou et al. reported an Au/CsPbBr_3 (18 μm)/ITO structure self-powered X-ray detector which obtained the sensitivity of $470 \mu\text{C Gy}_{\text{air}}^{-1} \text{cm}^{-2}$ at zero bias. They fabricated the CsPbBr_3 thick films through the multiple-times dissolution-recrystallization method[16]. W. Pan et al. reported a hot-pressed CsPbBr_3 quasi-monocrystalline thick film (240 μm) and a record sensitivity of $55,684 \mu\text{C Gy}_{\text{air}}^{-1} \text{cm}^{-2}$, surpassing all other X-ray detectors[17]. Due to these brilliant achievement by CsPbBr_3 X-ray detectors, it is expected that an application for highly sensitive X-ray imaging which enable medical diagnosis at a low dose rate, leading to reducing the risk of cancer. However, almost previous fabrication methods for CsPbBr_3 X-ray detectors were not suitable for the large area production. For X-ray imaging devices, large detection area equivalent to imaging area is essential because it is difficult to condense an X-ray by a lens in contrast to visible light. Therefore, a scalable method is required for the fabrication of thick CsPbBr_3 films.

Recently, we reported the fabrication of (101)-oriented CsPbBr_3 films with a thickness of up to 28 μm using a mist deposition method, which is suitable for the large area production[21]. Much thicker films (over 100 μm) are preferable to a highly sensitive X-ray detection. However, it is difficult to prepare such thick films due to the film exfoliation during a cooling process after the deposition. In this study, we employed a polymer as a buffer layer to prevent a CsPbBr_3 thick film from exfoliation and successfully obtained a 110- μm -thick CsPbBr_3 film. An X-ray detector based on the CsPbBr_3 thick film achieved a high sensitivity of $11,840 \mu\text{C Gy}_{\text{air}}^{-1} \text{cm}^{-2}$.

Table I. Comparison of the relevant device parameters of the X-ray detectors based on perovskite materials.

Material	Method	Thickness (μm)	X-ray (kV)	Electric Field (V mm^{-1})	Sensitivity ($\mu\text{C Gy}_{\text{air}}^{-1} \text{cm}^{-2}$)	Ref.
$\text{CH}_3\text{NH}_2\text{PbI}_3$ film	Spin-coating	0.6	N/A	0	25	[11]
$\text{CH}_3\text{NH}_2\text{PbBr}_3$ single crystal	Anti-solvent crystallization	2,000	N/A	0.05	80	[12]
$\text{CH}_3\text{NH}_2\text{PbBr}_3$ single crystal	Inverse temperature crystallization	2,000	8	47	21,000	[13]
$\text{CH}_3\text{NH}_2\text{PbI}_3$ thick film	Doctor blading	830	100	60	11,000	[14]
(CsFAMA)/ PbI_2 film	Spin-coating	0.45	35	890	98	[15]
CsPbBr_3 thick film	Multiple-times dissolution-recrystallization	18	35	110	1,700	[16]
CsPbBr_3 thick film	Hot-pressed	240	30	5.0	55,684	[17]
CsPbBr_3 thick film	Mist deposition	110	70	45.5	11,840	This work

EXPERIMENTAL DETAILS

Materials

Cesium bromide (CsBr , 99%) and lead bromide (PbBr_2 , 98%) were purchased from Tokyo Chemical Industry and Sigma-Aldrich, respectively. Dimethyl sulfoxide (DMSO, 99.0%) and *N, N*-dimethylformamide (DMF, 99.5%) were purchased from Fujifilm Wako Chemicals. CsPbBr_3 powder was synthesized from CsBr and PbBr_2 by reference to C. C. Stoumpos's solution method[19].

Preparation of CsPbBr_3 thick films

Pt-coated ITO substrates (named Pt substrates, size; $26 \times 20 \text{ mm}^2$) were cleaned by acetone, isopropanol and distilled water in ultrasonic bath for 10 min, respectively. Subsequently, the substrates were dried by an air blower. In order to avoid a film exfoliation, the Pt substrates were coated with a polymer using spin-coating method. CsPbBr₃ thick films were prepared on the Pt substrates with and without the polymer layer. The growth conditions of CsPbBr₃ are summarized in Table II. A precursor solution was prepared by dissolving 50 mM CsPbBr₃ powder in a solvent mixture of DMSO and DMF (6:4, volume ratio). Then CsPbBr₃ was deposited on the substrates using the mist deposition method. The carrier and dilution gas flow rate were set at 0.375 and 4.625 L min⁻¹, respectively. The substrate temperature was set at 150 °C optimized for the fabrication of highly (101)-oriented CsPbBr₃ films in our previous report[21]. In this study, CsPbBr₃ was deposited onto a reduced area of $26 \times 10 \text{ mm}^2$ by moving the substrate by 10 mm at a speed of 0.80 mm s⁻¹. The deposition cycle was determined to give thickness of about 100 μm. After the CsPbBr₃ deposition, the substrate temperature was slowly decreased to room temperature at the cooling rate of less than 2 °C min⁻¹.

Table II. Growth conditions of CsPbBr₃ thick films

Precursor, concentration	CsPbBr ₃ , 50 mM
Solvent	DMSO : DMF = 6 : 4 (volume ratio)
Carrier gas flow rate	N ₂ , 0.375 L min ⁻¹
Dilution gas, flow rate	N ₂ , 4.625 L min ⁻¹
Substrate temperature	150 °C
Stage speed, length	0.80 mm s ⁻¹ , 10 mm

Characterization and device fabrication

The surface and cross-sections of the films were observed with scanning electron microscopy (SEM; JSM-6510LV, JEOL). X-ray diffraction (XRD) spectra of CsPbBr₃ films were recorded using a PW 3040/60 X'Pert PRO with Cu-Kα radiation.

An X-ray detector with the configuration of tungsten (W)/CsPbBr₃/polymer/Pt substrate. Subsequently, a CsPbBr₃ thick film was deposited on a polymer-coated Pt substrate. Subsequently, a W electrode was deposited on the CsPbBr₃ film using ion sputtering coating. The device area of 0.25 cm² was determined by a metal mask.

Figure 1 shows the schematic illustration of X-ray detection measurements. The photoresponse characteristics of the X-ray detector were measured by a W target X-ray source. The tube voltage and tube current used in the measurement were 70 kV and 2.0 mA, respectively. The dose rate of the X-ray was 10 μGy_{air} s⁻¹ measured by an ionized chamber type survey meter. These measurements were performed in a dark room to exclude an effect of other photons such as visible light.

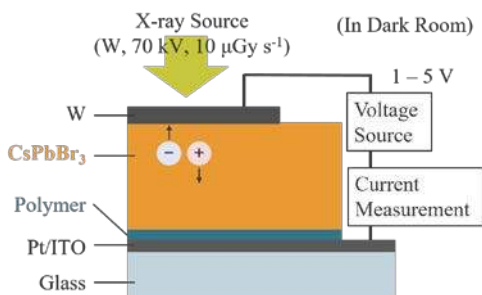


Figure 1. Schematic illustration of X-ray detection measurements.

RESULTS AND DISCUSSION

In our previous report, a 28- μm -thick CsPbBr_3 film was successfully formed on a Pt substrate using the mist deposition method[21]. Much thicker films (over 100 μm) are preferable to a highly sensitive X-ray detection. Then, the deposition cycle was increased to increase the thickness of a CsPbBr_3 thick film. Figure 2a shows the photographs of the obtained film on the Pt substrate. Unfortunately, many light orange speckles appeared on the film surface during the cooling process after the CsPbBr_3 deposition. The cross-sectional SEM image of the film (Figure 2b, c) revealed that the speckles corresponded to the exfoliation of the film. It seems that large stress was accumulated at the interface between the CsPbBr_3 film and the Pt substrate due to the difference of thermal expansion coefficient. The high thermal expansion coefficient of CsPbBr_3 ($1.2 \times 10^{-4} \text{ K}^{-1}$ [19]) makes it difficult to form a thick film on the Pt substrate without exfoliation. Therefore, a part of the Pt substrate was coated with a polymer as a buffer layer. Figure 2d shows the photograph of a CsPbBr_3 thick film prepared on the polymer-coated substrate. Unlike the CsPbBr_3 film directly prepared on the Pt substrate, a uniform orange film was obtained on the polymer layer without any speckles. The SEM images (Figure 2e) confirmed that a uniform 110- μm -thick CsPbBr_3 film was successfully obtained without exfoliation, as a result of inserting the polymer layer. As can be seen in figure 2f, columnar crystals grew even on the polymer layer. In addition, XRD patterns indicated that the CsPbBr_3 thick film was highly (101)-oriented. The columnar growth and the high (101)-orientation, corresponded to the results of our previous report[21], suggest that the CsPbBr_3 film has a high carrier mobility, leading to a highly sensitive X-ray detection.

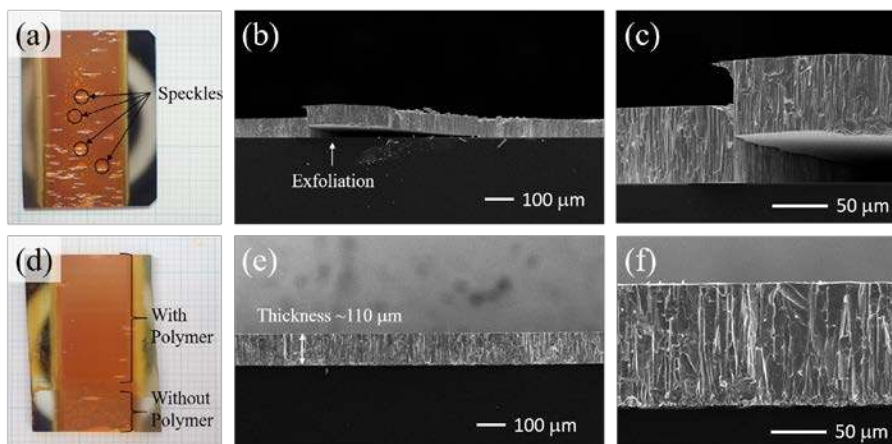


Figure 2. (a, d) Photographs and (b, c, e, f) cross-sectional SEM images of CsPbBr_3 thick films prepared on (a–c) a bare Pt substrate and (d–f) a polymer-coated Pt substrate.

An X-ray detector was fabricated by forming a W electrode onto the 110- μm -thick CsPbBr_3 film. Figure 3a shows the photoresponses to the X-ray with the dose rate of $10 \mu\text{Gy}_{\text{air}} \text{ s}^{-1}$ under bias voltages of 1–5 V. Under any bias voltages, the measured current

was pumped up by the X-ray irradiation, indicating that the X-ray detector could detect the X-ray. The sensitivity of the X-ray detector was calculated using the equation (1):

$$\text{Sensitivity} = (J_p - J_D)/G \quad (1)$$

where J_p , J_D , and G are the measured photocurrent density, dark current density, and the dose rate of $10 \mu\text{Gy}_{\text{air}} \text{s}^{-1}$. As shown in figure 3b, the sensitivity increased with increasing bias voltage and reached at $11,840 \mu\text{C Gy}_{\text{air}}^{-1} \text{cm}^{-2}$ under bias voltage of 5 V (45.5 V mm^{-1}). The sensitivity of our device ($11,840 \mu\text{C Gy}_{\text{air}}^{-1} \text{cm}^{-2}$) is much higher than that of the majority of other perovskite devices as shown in Table I. Moreover, this sensitivity is about 600 times higher than that of the currently commercial a-Se X-ray detectors working at a much higher field of $10,000 \text{ V mm}^{-1}$ ($20 \mu\text{C Gy}_{\text{air}}^{-1} \text{cm}^{-2}$)[22].

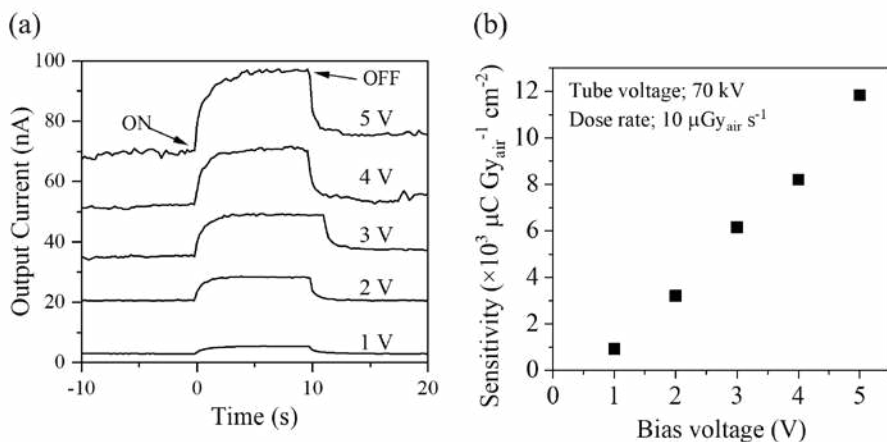


Figure 3. (a) X-ray responses and (b) sensitivities of the W/CsPbBr₃/polymer/Pt detector under various bias voltage of 1–5 V.

CONCLUSIONS

In conclusion, we employed a polymer as a buffer layer to prevent a CsPbBr₃ film from exfoliation and successfully fabricated an X-ray detector based on a 110-um-thick CsPbBr₃ film using a scalable solution deposition method (mist deposition method). The detector demonstrated a high sensitivity of $11,840 \mu\text{C Gy}_{\text{air}}^{-1} \text{cm}^{-2}$, which is about 600 times higher than that of currently commercial a-Se X-ray detectors. Our investigation has provided a scalable method to fabricate X-ray detectors based on CsPbBr₃ thick film which achieve a high sensitivity.

ACKNOWLEDGMENTS

This work was supported by Hamamatsu Photonics K. K. and JSPS KAKENHI (Grant No. 17K18988, 18K18943).

REFERENCES

- [1] A. Kojima, K. Teshima, Y. Shirai, and T. Miyasaka, “Organometal Halide Perovskites as Visible-Light Sensitizers for Photovoltaic Cells,” *J. Am. Chem. Soc.*, vol. 131, no. 17, pp. 6050–6051, May 2009.
- [2] M. Feng, S. You, N. Cheng, and J. Du, “High quality perovskite film solar cell using methanol as additive with 19.5% power conversion efficiency,” *Electrochim. Acta*, vol. 293, pp. 356–363, 2019.
- [3] J. Duan *et al.*, “Spray-assisted deposition of CsPbBr₃ films in ambient air for large-area inorganic perovskite solar cells,” *Mater. Today Energy*, vol. 10, pp. 146–152, Dec. 2018.
- [4] M. Saliba *et al.*, “Cesium-containing triple cation perovskite solar cells: improved stability, reproducibility and high efficiency,” *Energy Environ. Sci.*, vol. 9, no. 6, pp. 1989–1997, 2016.
- [5] J. Liang *et al.*, “All-Inorganic Perovskite Solar Cells,” *J. Am. Chem. Soc.*, vol. 138, no. 49, pp. 15829–15832, Dec. 2016.
- [6] H. T. Pham, T. Duong, W. D. A. Rickard, F. Kremer, K. J. Weber, and J. Wong-Leung, “Understanding the Chemical and Structural Properties of Multiple-Cation Mixed Halide Perovskite,” *J. Phys. Chem. C*, vol. 123, no. 43, pp. 26718–26726, Oct. 2019.
- [7] M. I. Saidaminov *et al.*, “Inorganic Lead Halide Perovskite Single Crystals: Phase-Selective Low-Temperature Growth, Carrier Transport Properties, and Self-Powered Photodetection,” *Adv. Opt. Mater.*, vol. 5, no. 2, p. 1600704, Jan. 2017.
- [8] J. Mater *et al.*, “In situ formation of CsPbBr₃/ZnO bulk heterojunctions towards photodetectors with ultrahigh responsivity,” *J. Mater. Chem. C*, 2018.
- [9] T. Yang, F. Li, and R. Zheng, “Recent Progress on Cesium Lead Halide Perovskites for Photodetection Applications,” *ACS Appl. Electron. Mater.*, vol. 1, no. 8, pp. 1348–1366, Aug. 2019.
- [10] C. Li *et al.*, “Enhanced photoresponse of self-powered perovskite photodetector based on ZnO nanoparticles decorated CsPbBr₃ films,” *Sol. Energy Mater. Sol. Cells*, vol. 172, no. June, pp. 341–346, Dec. 2017.
- [11] S. Yakunin *et al.*, “Detection of X-ray photons by solution-processed lead halide perovskites,” *Nat. Photonics*, vol. 9, no. 7, pp. 444–449, Jul. 2015.
- [12] H. Wei *et al.*, “Sensitive X-ray detectors made of methylammonium lead tribromide perovskite single crystals,” *Nat. Photonics*, vol. 10, no. 5, pp. 333–339, May 2016.
- [13] W. Wei *et al.*, “Monolithic integration of hybrid perovskite single crystals with heterogenous substrate for highly sensitive X-ray imaging,” *Nat. Photonics*, vol. 11, no. 5, pp. 315–321, May 2017.
- [14] Y. C. Kim *et al.*, “Printable organometallic perovskite enables large-area, low-dose X-ray imaging,” *Nature*, vol. 550, no. 7674, pp. 87–91, Oct. 2017.
- [15] L. Basiricò, S. P. Senanayak, A. Ciavatti, M. Abdi-Jalebi, B. Fraboni, and H. Sirringhaus, “Detection of X-Rays by Solution-Processed Cesium-Containing Mixed Triple Cation Perovskite Thin Films,” *Adv. Funct. Mater.*, vol. 29, no. 34, p. 1902346, Aug. 2019.
- [16] Z. Gou *et al.*, “Self-Powered X-Ray Detector Based on All-Inorganic Perovskite Thick Film with High Sensitivity Under Low Dose Rate,” *Phys. status solidi – Rapid Res. Lett.*, vol. 13, no. 8, p. 1900094, Aug. 2019.

- [17] W. Pan *et al.*, “Hot-Pressed CsPbBr₃ Quasi-Monocrystalline Film for Sensitive Direct X-ray Detection,” *Adv. Mater.*, vol. 1904405, p. 1904405, Sep. 2019.
- [18] R. Fu, W. Zhou, Q. Li, Y. Zhao, D. Yu, and Q. Zhao, “Stability Challenges for Perovskite Solar Cells,” *ChemNanoMat*, vol. 5, no. 3, pp. 253–265, Mar. 2019.
- [19] C. C. Stoumpos *et al.*, “Crystal Growth of the Perovskite Semiconductor CsPbBr₃: A New Material for High-Energy Radiation Detection,” *Cryst. Growth Des.*, vol. 13, no. 7, pp. 2722–2727, Jul. 2013.
- [20] Y. He *et al.*, “High spectral resolution of gamma-rays at room temperature by perovskite CsPbBr₃ single crystals,” *Nat. Commun.*, vol. 9, no. 1, p. 1609, Dec. 2018.
- [21] Y. Haruta, T. Ikenoue, M. Miyake, and T. Hirato, “Fabrication of (101)-oriented CsPbBr₃ thick films with high carrier mobility using a mist deposition method,” *Appl. Phys. Express*, vol. 12, no. 8, p. 085505, Aug. 2019.
- [22] S. O. Kasap, “X-ray sensitivity of photoconductors: application to stabilized a-Se,” *J. Phys. D. Appl. Phys.*, vol. 33, no. 21, pp. 2853–2865, Nov. 2000.